Mechanisms of housedust-induced toxicity in primary human corneal epithelial cells: oxidative stress, proinflammatory response and mitochondrial dysfunction

Ping Xiang[1], Rui-Wen He[1], Yong-He Han[1], Hong-Jie Sun[1], Xin-Yi Cui[1], and Lena Q. Ma[1,2,*]

[1] State Key Laboratory of Pollution Control and Resource Reuse, School of the Environment, Nanjing University, Nanjing 210046, People's Republic of China

[2] Soil and Water Science Department, University of Florida, Gainesville, Florida 32611, United States

*Corresponding author, State Key Laboratory of Pollution Control and Resource Reuse, School of the Environment, Nanjing University, Nanjing 210046, People's Republic of China, Tel./fax: +86 025 8968 0631, E-mail: lqma@ufl.edu

Abstract

Human cornea is highly susceptible to damage by dust. Continued daily exposure to housedust has been associated with increasing risks of corneal injury, however, the underlying mechanism has not been elucidated. In this study, a composite housedust sample was tested for its cytotoxicity on primary human corneal epithelial (PHCE) cells, which were exposed to dust at 5–320 μg/100 μL for 24 h. PHCE cell viability showed a concentration-dependent toxic effect, attributing to elevated intracellular ROS. Moreover, when exposed at >20–80 μg/100 μL, dust-induced oxidative damage was evidenced by increased malondialdehyde and 8-hydroxy-2-deoxyguanosine (1.3–2.3 folds) and decreased antioxidative capacity (1.6–3.5 folds). Alteration of mRNA expression of antioxidant enzymes (*SOD1*, *CAT*, *HO-1*, TRXR1, GSTM1, *GSTP1*, and *GPX1*) and pro-inflammatory mediators (*IL-1β, IL-6, IL-8, TNF-α, and MCP-1*) were also observed. Furthermore, the mitochondrial transmembrane potential was dissipated from 9.2 to 82%. Our results suggested that dust-induced oxidative stress probably played a vital role in the cytotoxicity in PHCE cells, which may have contributed to dust-induced impairment of human cornea.

Keywords: Housedust; primary human corneal epithelial cells; oxidative stress; inflammation; mitochondrial dysfunction

1. Introduction

Epidemiological studies have linked human health issues, including respiratory, allergenic, and ocular surface diseases with exposure to housedust (Maertens et al., 2004; Torricelli et al., 2014). Housedust is a complex heterogeneous mixture of particles of different sources, which contains both harmful microbes and various contaminants (Fang and Stapleton 2014; Li et al., 2014; Pitkäranta et al., 2008). The contaminants in housedust are probably responsible for the adverse health effects. Accumulating evidence demonstrated that organic pollutants such as phosphorus flame retardants (PFRs) and phthalic acid esters (PAEs) in indoor dust were positively associated with human diseases (Betts 2015; Kolarik et al., 2008; Meeker and Stapleton 2010; He et al. 2015). Heavy metals in dust have also attracted attentions due to their persistence in the environment and potential adverse health effect on human health (Yu et al., 2014).

People spend long time indoors, especially for young children. It has been estimated that ~51 mg housedust can be absorbed by adults and 28 mg for kids (Hawley 1985). Thus, it is important to address the potential human health risk associated with exposure to dust. Most studies addressed effects of indoor dust on human respiratory and cardiovascular system, but few investigations focus on dust-induced damage on eye surface. Human eyes are sensitive organ, which are exposed to ambient air every day and are susceptible to damage by housedust. Epidemiological data showed that the air pollution and airborne particulate matters in household significantly impacts the eyes, especially ocular surface such as conjunctiva and cornea (Saxena et al., 2003). Strong association (r= 0.62) between the number of outpatient visits for eye surface diseases and airborne particulate matter exposure

63 levels has been observed (Mimura et al., 2014). Gupta et al. (2007) also indicated that people
64 exposed to high air pollutants are linked to high incidence of subclinical ocular surface
65 disorders. Changes in foam formation in the eyes (Franck and Skov 1989) and tear film
66 stability were affected by dust exposure (Pan et al., 2000).

67 The corneal epithelium, the outermost cell layers of the eye, serves as the mechanical
68 barrier to environmental agents including dust to minimize interior damage (Black et al.,
69 2011; Leong and Tong 2015). Exposure to indoor dust, even at concentrations of normal
70 indoor environments led to corneal epithelium defects and breakup time decrease (Mølhave et
71 al., 2002). House dust exposure can also irritates human corneal epithelium (HCE) and
72 damage its histological structure (Cao et al., 2015), which may lead to impaired vision and
73 eventual blindness (Cullen 2002; Lu et al., 2001). Therefore, dust-induced corneal diseases is
74 of concern and warrants more investigation (West et al., 2013; Wolkoff et al., 2003).

75 To elucidate the underlying molecular mechanism of dust-induced toxicity in human eyes,
76 various human cell line models have been employed including cancer cells and immortalized
77 cell lines (Kang et al., 2010a; Riechelmann et al., 2007). However, recent study showed
78 different pattern and magnitude of cytokine expression from immortalized and primary HCE
79 (PHCE) cells responding to particulate matter (Ekstrand-Hammarstrom et al., 2013), with
80 PHCE showing higher sensitivity than immortalized cell lines (De Saint Jean et al., 2004).
81 Others also demonstrated that immortalized human epithelial cell lines have lost or changed
82 some features after long term *in vitro* culture under changed physiological conditions (Proulx
83 et al., 2004). In short, the differences observed between primary cells and immortalized cell
84 lines suggests it is important to use primary cultures to assess contaminant toxicity (Cree and

Andreotti 1997).

Oxidative stress is a vital molecular mechanism of environment-mediated corneal epithelium injury, attributing to the localized production of ROS by HCE cells (Lee et al., 2014). Several studies have demonstrated that increase of ROS directly suppressed several antioxidant enzymes including catalase (CAT), and superoxide dismutase (SOD) in HCE cells (Black et al., 2011; Čejková et al., 2004). Moreover, ROS can also damage DNA and oxidize lipids and key proteins, resulting in excessive production of inflammatory mediators, malondialdehyde and 8-hydroxy-2-deoxyguanosine, causing toxic effects (Cejkova et al., 2000; Ye et al., 2012). Excessive ROS induces the production of proinflammatory mediators, contributing to many corneal inflammatory diseases such as corneal inflammation, dry eye disease, and bullous keratopathy (Shoham et al., 2008). Nevertheless, the potential role of oxidative damage induced by housedust in PHCE cells has not been investigated.

In this study, we hypothesized that oxidative stress was responsible for housedust-induced cytotoxicity in PHCE cells. We tested the impact of housedust on PHCE cells after exposure to various dust concentrations for 24 h. The specific objectives of this study were: (1) to investigate the toxicity of PHCE cells after exposure to housedust, and (2) to evaluate dust-induced toxicity mechanisms by evaluating the oxidative toxicity and inflammatory mediator expression, and mitochondrial transmembrane potential depolarization of PHCE cells after exposure to housedust. This is the first study using PHCE cells to test dust-induced toxicity and its associated mechanisms.

2. Materials and methods

2.1 Chemicals and reagents

Cell culture reagents and plates were obtained from Life Technologies Inc. (CA, USA) and Corning Inc. (NY, USA). CCK-8 cell viability assay kit, malondialdehyde (MDA) assay kit, and total antioxidant capacity assay kit were purchased from Nanjing Jiancheng Bioengineering Institute (Nanjing, China). JC-1 mitochondrial membrane potential assay kit, reactive oxygen species assay kit (DCFH-DA), RNase-Free DNase I and cell lysis buffer were purchased from Beyotime Institute of Biotechnology (Haimen, China). Chemical standards were purchased from Aladdin Industrial Corporation (Shanghai, China) and J&K Scientific (Shanghai, China) with purity> 98% including five phthalic acid esters (PAEs) [dimethyl phthalate-(DMP), diethyl phthalate (DEP), di-n-butyl phthalate (DBP), benzyl butyl phthalate (BBP) and di-2-ethylhexyl phthalate (DEHP)] and five PFRs [tris(2-chloroethyl) phosphate (TCEP), tris(chloroisopropyl) phosphate (TCPP), tris(1,3-dichloro-2-propyl) phosphate (TDCPP), triphenyl phosphate (TPP), and 2-ethylhexyl diphenyl phosphate (EHDPP)]. Other chemicals were obtained from Sigma-Aldrich, Inc. (MO, USA).

2.2 Sampling and characterization of indoor dust

Sixteen indoor dust samples were collected from Nanjing, China. In each house, dust was obtained from air conditioner filter by a vacuum cleaner with a paper bag (Philips Fc8222, China). All dust samples were freeze-dried, and sieved through nylon sieve (<100 μm) to remove fibrous fragments and large particles, it was then mixed into one composite sample and stored in clean aluminum foil at –20℃ until analysis. For preparation of dust suspension,

200 mg of dust were suspended into 40 mL Hank's balanced salt solution containing 3% antibiotic-antimycotic solution and sonicated at 4°C for 15 min 4 times and vortexed before exposure to the cells.

Concentrations of heavy metals including As, Pb, Cr, Cd, Cu, Zn, Ni, Sb, Ti, and Mn were determined by inductively coupled plasma mass spectrometry (ICP-MS) (NexION300X, PerkinElmer) after digestion using USEPA Method 3050B. Total concentrations of PAEs and PFRs were quantified (Guo and Kannan 2011). Sample of 200 mg was extracted with 20 mL n-hexane in ultrasonic bath (SCOENTZ, SB-800 DTD, China) for 30 min three consecutive times. The extracts were collected after centrifugation at 3000 rpm for 5 min, and filtrated through anhydrous sodium sulfate for dehydration into 150 mL flask bottle. The combined extract was concentrated to near dryness by rotatory evaporimeter (IKA®RV10, Germany), and then reconstituted in 2 mL n-hexane, which was transferred to 2 mL amber vials through 0.45 mm Nylon filter (ANPEL, China) and stored at −20°C until analysis. Ten organic compounds including five PAEs and five PFRs were detected using gas chromatography coupled with mass spectrometry (Agilent Technologies,7890A) (GC-MS) in selective ion-monitoring mode. After carbonate carbon was removed using 0.5 M HCl, total organic carbon (TOC) contents in dust samples were also measured using element analyzer (vario TOC select, Elementar, Germany).

The concentration of endotoxin (lipopolysaccharide, LPS) in dust sample was tested using Kinetic turbidimetric LAL assay kit (Chines Horseshoe Crab Reagent Manufactory, CO., Ltd., Xiamen, China). Endotoxin concentrations were expressed in EU per milligram of dust.

2.3 Cell culture and exposure to housedust

Primary human corneal epithelial (PHCE) cells originally isolated from corneas of a healthy donor were obtained from the Eye Bank of Wenzhou Medical University. They were cultured in DMEM medium containing high glucose (4.5 g/L), fetal bovine serum (10%), epidermal growth factor (10 ng/mL) and 1% antibiotic-antimycotic solution in an incubator with 5% CO_2 at 37°C. For the following studies, PHCE cells were seeded into 6/24/96-well plates and cultured for 24 h to reach ~80% confluence. Subsequently, the culture medium was changed and HCE cells were incubated with fresh medium containing 5 to 320 μg/100 μL of housedust suspension for 24 h.

2.4 Analysis of cell viability and intracellular ROS

To test the effect of dust on cell viability, PHCE cells were seeded in a 96-well plate at density of 1×10^4 cells/100 μL/well. After 24 h exposure, the cell morphology was observed via an inverted microscopy (TS-100, Nikon, Japan). Cell viability was measured by CCK-8 cell viability assay kit.

Changes in intracellular ROS level after dust exposure was detected using a well-characterized probe 2',7'-dichlorofluorescein diacetate (DCFH-DA). DCFH-DA is permeated into cytoplasm and hydrolyzed into non-fluorescent DCFH. Under ROS, DCFH is converted into fluorescent dichlorofluorescein. Briefly, PHCE cells were cultured with control medium and different concentrations of dust in a 24-well plate for 24 h. Then, cell culture medium was aspirated and washed by HBSS. DCFH-DA was added into cells for 30 min in dark. Subsequently, the fluorescence image was visualized by inversed fluorescent microscopy (Eclipse Ti-U, Nikon, Japan).

2.5 Malondialdehyde (MDA), 8-Hydroxy-2-deoxyguanosine (8-OHdG) and total

antioxidant capacity (T-AOC)

The level of MDA, a marker of toxic byproduct of lipid peroxidation was detected using MDA assay kit (TBA method). Briefly, PHCE cells were seeded into a 24-well plate at 4×10^5 cells/well overnight, and then exposed to dust for 24 h. Following exposure, cell culture medium was aspirated and the cells were gently rinsed with ice-cold HBSS twice and lysed with cell lysis buffer. The lysate was centrifuged at 10,000 g and 4°C for 10 min to remove debris. MDA concentrations and protein contents were determined in the clear supernatant.

Another oxidative stress marker 8-OHdG was determined to evaluate oxidative DNA damage using enzyme linked immunosorbent assays (ELISA) (CUSABIO, China). In brief, PHCE cells were replanted into a 24-well plate at 4×10^5 cells/well overnight, then exposed to dust for 24 h. Subsequently, cell culture supernatant was collected, centrifuged, and tested for 8-OHdG secretion.

The T-AOC of HCE cells was evaluated by a commercial kit. T-AOC was evaluated by reduction of Fe^{3+}-TPTZ to the blue Fe^{2+}-TPTZ complex, whose optical density was determined at 520 nm. One unit (U) of T-AOC was defined as the amount of antioxidant power which increased optical absorbance by 0.01 at 37°C.

2.6 Quantitative RT-PCR and mitochondrial membrane potential

To better understand dust-induced oxidative stress, PHCE cells were replanted into a 6-well plate at 1×10^6 cells/well overnight, and then exposed to dust for 24 h. PHCE cells were harvested and analyzed for the expression levels of antioxidative enzymes and pro-inflammatory mediator genes based on total RNA of PHCE cells, which were extracted using RNAiso Reagent (TaKaRa Biotech. Co., Japan). RNase-Free DNase I was used to

remove contaminated DNA. The quality of RNA was measured using a NanoDrop 2000 Spectrophotometer (Thermo Fisher Scientific Inc., USA). cDNA synthesis was performed via PrimeScript RT reagent kit (TaKaRa Biotech. Co., Japan). Real-time quantitative polymerase chain reaction (RT-qPCR) was conducted using SYBR® Premix Ex Taq Ⅱ (Tli RNaseH Plus) (TaKaRa Biotech. Co., Japan) to analyze the expression levels of antioxidative enzymes and proinflammatory mediator genes in a CFX Connect™ Real-Time PCR detection system (Bio-Rad, CA, USA) at the following cycling conditions: 95°C for 2 min, followed by 40 cycles of 95°C for 5 s and 60°C for 30 s. After the last reaction, the melting curve was also done from 65 to 95°C with 0.5°C s^{-1} increments to exclude unspecific amplification. For each sample, relative mRNA expression was normalized to housekeeping gene *β-Actin*. The fold changes of target genes were calculated by $2^{-\Delta\Delta CT}$ method. The specific primers were obtained from Harvard PrimerBank (Wang et al., 2012) (Table S1).

Mitochondria is one of the most important cytoplasmic organelles to supply most of the necessary energy for cellular activities and functions. To detect whether dust-induced oxidative stress altered mitochondrial function, a well-characterized JC-1 probe was employed to evaluate the loss of mitochondrial membrane potential ($\Delta\Psi m$). Briefly, PHCE cells were seeded into a 24-well plate at 4×10^5 cells/well overnight, and then exposed to dust for 24 h. After exposure, cell culture medium was exchanged with 500 μL fresh medium containing 250 μL of JC-1 working staining solution and incubated at 37℃ for 20 min. Subsequently, cells were washed twice with HBSS, and images were captured by inversed fluorescent microscopy (Eclipse Ti-U, Nikon, Japan). Additionally, the changes in color was quantified and analyzed by BD LSRFortessa cell analyzer (BD Biosciences, USA). The

fluorescence intensity of increasing green indicates mitochondrial depolarization. Carbonyl cyanide 3-chlorophenylhydrazone at 10 μmol/L was served to treat cells as a positive control.

2.7 Statistical analysis

All experiments were carried out in triplicate. Statistical analyses were conducted using one-way ANOVA by PASW Statistics Version 18 (SPSS Inc., USA) and Graphpad Prism Version 6 (Graphpad Software, USA). Significant differences were set at $\alpha = 0.05$.

3. Result

3.1 Housedust characteristics and cell morphology and viability

Table S2 shows the characteristics of composite housedust sample. The average TOC content was typical at 20.4%. Among the five PAEs, DEHP was the most abundant at 562 mg/kg and followed by DBP at 170 mg/kg, while the other three compounds were similar but with much lower concentrations at < 0.77 mg/kg. For the five PFRs, the concentration of TECP (46.8 mg/kg) was much higher than other four compounds, which was at < 1.84 mg/kg. Among the metals measured (mg/kg), Zn (2073), Mn (389), Cu (323) and Pb (241) were the most abundant in the sample. The content of endotoxin in dust sample was 54.8 EU/mg (Table S2).

As an important inductor of cytotoxicity, the cell morphology after dust exposure was recorded (Fig. 1). The typical polygonal and cobblestone appearance of confluent HCE cell monolayer was clear in the control and low exposure group (5 μg/100 μL) (Fig. 1AB). However, cells became spindle shape with increasing dust concentration (Fig. 1CD) and cell density was significantly decreased at high exposure (> 160 μg/100 μL) (Fig. 1GH).

In addition to cell morphology, we also measured cell. PHCE cell viability was affected

by dust in a concentration-dependent manner. At low concentration, housedust showed little effect on cell viability (Fig. 2A). At higher concentrations (>160 μg/100 μL), the cell viability was reduced by >50%. Based on the fitted curve, the LC_{50} value was 128 μg/100 μL (95% confidence interval at 89.5 to 183 μg/100 μL) (Fig. 2B).

3.2 Dust-induced oxidative stress characterized by elevations of ROS, MDA and 8-OHdG

To determine the underlying mechanisms of dust-induced cytotoxicity, we evaluated the effects of dust on PHCE cells by monitoring their ability to generate intracellular ROS via DCFH-DA probe in conjunction with inversed fluorescent microscopy. The PHCE cells after exposing to 5 μg/100 μL showed slight increase in fluorescence intensity (11±0.9%) compared to control group (8.1±1.2%) (Fig.3 A-F''). Increased exposure caused a concentration-dependent increase in ROS production. More than 95% green fluorescent cells was evident after exposure to 160 μg/100 μL dust (Fig. 3G). MDA, a byproduct of lipid peroxidation was used as another indicator of oxidative stress. Although there was no effect at 5 μg/100 μL, MDA concentrations were significantly elevated from 2.33 to 4.57 mmol/mg protein in PHCE cells at dust concentrations >20–320 μg/100 μL, suggesting aggravation of lipid peroxidation with increasing dust concentration (Fig. 3H). The production of 8-OHdG as a measure of oxidative-stress induced DNA damage was also analyzed. After exposure, 8-OHdG level in cells exposed to 5 μg/100 μL was 223±12.2 pg/mL, which was similar to the control cells at 214±6.50 pg/mL (Fig. 3I). However, 8-OHdG contents were remarkably increased to 400±38.8 pg/mL upon exposure to higher dust concentration at 80 μg/100 μL. Interestingly, although lipid peroxidation and DNA damage were significantly increased at 20

μg/100 μL dust treatment, we did not observe statistic difference in PHCE cell viability at this concentration.

3.3 Dust altered T-AOC and mRNA expression of antioxidant enzymes

To test responses of antioxidant system of PHCE cells to dust-induced oxidative stress, we examined the changes of total antioxidant capacity (T-AOC) upon dust exposure. T-AOC was significantly increased to 25.2±1.1 U/mg protein at 5 μg/100 μL dust, which was 1.4-fold higher than the control group at 18.3±2.57 U/mg protein ($p<0.05$) (Fig. 4A). However, it then reduced to 5.20±1.60 U/mg protein upon exposure to 320 μg/100 μL dust (Fig. 4A).

Potential mechanisms of cellular action of dust-induced oxidative stress may include their ability to modulate expression of enzymes involved in antioxidant defenses including primary and secondary antioxidant enzymes. Dust exposure of PHCE cells significantly decreased mRNA expression of primary antioxidants-superoxide dismutase *(SOD1)* and catalase (*CAT*) (Fig. 4BC*)*. For secondary antioxidant enzymes, remarkable upregulation of thioredoxin reductase *(TRXR1)* (Fig. 4D), glutathione S-transferase mu 1 *(GSTM1)* and *HO-1* (Fig. 4GE) mRNA were observed, most effective at 5 and 20 μg/100 μL. Glutathione S-transferase pi *(GSTP1)* and glutathione peroxidase 1 *(GPX1)* (Fig. 4FH) mRNA expressions were not altered by dust at >20 μg/100 μL, however, they decreased by 5.6- and 4.8-folds at 320 μg/100 μL.

3.4 Dust alters mRNA levels of inflammatory mediators

Several investigations have identified links between elevations in biomarkers of oxidative stress and inflammatory response characterized by the production of proinflammatory

mediators including *IL-1β, IL-6, IL-8,* tumor necrosis factor α *(TNF-α),* transforming growth factor-β *(TGF-β),* regulated upon activation normal T cell expressed and secreted *(RANTES),* and monocyte chemoattractant protein-1 *(MCP-1)*. Dust caused a dose-dependent increase mRNA expression of *IL-1β, IL-6* and *IL-8* (Fig. 5ABC). The highest upregulation of 3.7-, 14- and 5.6- folds were observed at 80, 320, and 20 μg/100 μL. Significantly increased mRNA expression of *TNF-α* and *MCP-1* at 2.7–3.7 folds were observed in 5 μg/100 μL dust (Fig. 5EG). However, 3-fold down-regulation in *TNF-α, MCP-1,* and *RANTES* was evident at > 20 μg/100 μL (Fig. 5H) while *TGF-β* mRNA expression was decreased 0.9-4.9 folds in a dose-dependent manner (Fig. 5F).

3.5 Dust induced loss of mitochondrial transmembrane potential

Accumulating evidence demonstrated that changes in the mitochondrial membrane potential (ΔΨm) was a subsequent event of oxidative stress. In this study, we investigated dust-triggered ΔΨm in PHCE cells. After exposure, PHCE cells exhibited an elevated green fluorescence intensity (Fig. 6C''-F'') and an attenuated red fluorescence signal (Fig. 6C'-F') in a dose-dependent manner. The percentage of fluoresced green reached 9.2±2.1, 19±3.9, 59±2.5, and 82±8.4% in PHCE cells at 5, 20, 80, and 320 μg/100 μL (Fig. 6G), which was correlated to ROS production (Fig. 6H).

4. Discussion

Our results showed the involvement of oxidative stress in dust-induced cytotoxicity in PHCE cells, which was supported by reduced cell viability (Fig. 2), elevated biomarkers of oxidative stress (Fig. 3), altered antioxidant enzyme levels (Fig. 4) and proinflammatory mediators mRNA expression (Fig. 5), and loss of mitochondrial membrane potential (Fig. 6).

Indoor dust concentrations vary widely, ranging from < 10 to 3200 μg/m^3 (Mølhave et al., 2000). Recently, reconstituted HCE tissue was exposed to housedust at concentrations of 500, 1500, and 3000 μg/100 μL for 24 h, which caused elevation of IL-1β and IL-8, reduction of HCE viability (Cao et al., 2015). However, few studies focused on the effects of lower dust concentration on HCE cells, so we used lower concentrations of 5 μg/100 μL and six other concentrations (10, 20, 40, 80, 160, and 320 μg/100 μL) at 2-fold increments.

Cell viability is a vital criteria in evaluating cellular responses to contaminants, which reflect metabolic activities, cell survival and cell death. Previous research showed that housedust influenced cytotoxicity and mutagenicity to many cancer cells and immortalized cell lines (e.g., human HepG2 and lung epithelial cells) (Kang et al., 2010a; Riechelmann et al., 2007). However, mounting evidence indicated that cell lines lose some characteristics over time, as a result, they showed low sensibility to stimuli compared to primary cultures (De Saint Jean et al., 2004). To accurately assess the potential cytotoxicity of housedust on corneal epithelium, PHCE cells were employed to minimize artifact since they more closely simulate *in vivo* condition. However, to our knowledge, there are no accurate data on housedust-induced toxicity in HCE cells. In this study, PHCE cells morphology was changed from typically polygonal appearance to spindle shape after dust exposure (Fig. 1), suggesting epithelial-mesenchymal transition was initiated (Fischer and Agrawal 2015). In our study, dust at < 20 μg/100 μL seemed insufficient to compromise cell viability. At > 40 μg/100 μL, increased cell mortality was evident with increasing dust concentrations. Cao et al (2015) reported HCE viability was significantly decreased at > 1500 μg/100 μL. One possible explanation was that HCE cell monolayer in this study was more sensitive to stratified HCE

cells.

The LC_{50} of dust on PHCE cells was 128 μg/100 μL, which was higher than those reported for indoor dust concentrations (<10 to 3200 μg/m^3) (Mølhave et al., 2000). However, exposing to office dust at concentrations of normal indoor environments (136 and 390 μg/m^3) led to corneal epithelium defects and breakup time decrease in humans (Mølhave et al., 2002). To further study the underlying mechanism of dust-induced cytotoxicity in PHCE cells, we selected 4 dust concentrations including 5, 20, and 80 μg/100 μL (<LC_{50}), and 320 μg/100 μL (>LC_{50}).

The elevations of ROS, MDA, and 8-OHdG production indicated dust-induced oxidative stress may have caused cytotoxicity in PHCE cells (Fig. 3). ROS are formed by incomplete electron reduction of oxygen, which participate in molecular signaling transduction and regulate pivotal cellular events (Apel and Hirt 2004). It has been documented that oxidative stress induced by elevated ROS is involved in dysfunction of corneal epithelium (Shoham et al., 2008). A number of studies reported that elevated contaminants including metals, PAEs and PFRs were positively associated with ROS level (Liu et al., 2001; Rusyn et al., 2001; Wei et al., 2009). The metals, PAEs, and PFRs in the dust may have contributed to elevated extracellular ROS production in the PHCE cells (Table S2).

Enhanced ROS disrupts the balance in oxidant-antioxidant systems in cells. The antioxidant enzymes (e.g., SOD, CAT, and GSTP1) and an array of antioxidants (e.g., glutathione, ceruloplasmin and ascorbic acid) are always ready to detoxify the reactive intermediates or repair the resulting damage in biological system. T-AOC as a biomarker of overall antioxidant capacity of organisms provides more relevant biological information

compared to that using individual component as it considers the synergetic action of all antioxidants in cells. In our study, we found elevated T-AOC in PHCE cells even at low dust concentration of 5 μg/100 μL, indicating an adaptive cytoprotective response to foreign stimulation (Black et al., 2011). However, the continuous production of ROS may exceed the capacity of cellular antioxidant defenses, leading to decreased T-AOC. An important molecular feature of cellular responses to oxidative stress is to modulate expression of certain genes in antioxidant enzymes. The SOD1 and CAT are important primary antioxidant enzymes to scavenge superoxide anion in the corneal epithelium, which are generally regulated by oxidative stress. In this study, mRNA expression for *SOD1* and *CAT* was not affected by dust until at concentrations >20 μg/100 μL. This may be because at lower concentration, other enzymes probably maintained the antioxidant defenses in PHCE cells. HO-1, a rate-limiting enzyme catalyzing the degradation of pro-oxidant heme, serves as an antioxidant protein in response to oxidative stress. The elevated mRNA expression of *HO-1* in PHCE cells was in agreement with literature that ambient exposure to air particles increased *HO-1* gene expression in human alveolar macrophages and airway epithelial cells (Becker et al., 2005). TRXR-1, an antioxidant of the thioredoxin system catalyzing the NADPH-dependent reduction of thioredoxin and GSTM1against cellular DNA from oxidative damage, plays an important role in control of cellular redox regulation (Wu et al., 2012). Our results clearly showed that both *HO-1* and *GSTM1* were induced after 24 h exposure to dust at >20 μg/100 μL, which was consistent with the report that UV-induced oxidative stress increased *GSTM1* and *HO-1* mRNA expression in PHCE cells (Black et al., 2011). Increased mRNA expression of *HO-1*, *TRXR1* and *GSTM1* after dust exposure may be

an important molecular mechanism for PHCE cells to alleviate oxidative stress and mitigate dust-induced corneal injury. However, all antioxidant enzymes were significantly down-regulated at > 80 μg/100 μL (Fig. 4). Higher dust exposure increased the contact of dust and cells, inducing greater physical stress, which probably suppressed antioxidant enzyme genes expression, resulting in more cell mortality (Figs.1 & 2).

Oxidative stress can directly activate the transcription factors including NF-κB and AP-1, resulting in the transcription of proinflammatory mediators involved in interleukins (e.g., *IL-6,* *IL-8,* and *IL-1β*) and other cytokines (e.g., MCP-1, and *TNF-α*) (Reuter et al., 2010). Oxidative stress is involved in many corneal inflammatory diseases such as corneal inflammation and dry eye disease, (Cejka and Cejkova 2015). The mRNA expressions of *IL-6,* *IL-8,* and *IL-1β* were upregulated along with ROS production in this study, indicating dust-induced oxidative stress also elicited inflammatory responses, which may be attributed to endotoxin and other contaminants in dust (Spilak et al., 2015). IL-1β acts as a key mediator in the pathogenesis of eye diseases (Tseng et al., 2013), which could significantly promote the release of IL-6, IL-8 and MCP-1 in HCE cell lines (Cavet et al., 2011). IL-6 is involved in acute systemic inflammations and corneal epithelial wound (Nishida et al., 1992). IL-8 and MCP-1, as chemotactic signals attracting monocytes into the injury and infection site participate corneal leukocytic infiltration (Elner et al., 1991). However, our results were different from Kang et al. (2010b) who reported that dust induced both up-regulation and down-regulation of *IL-8* and *IL-1β* mRNA expression in human premonocytic cell line (Kang et al., 2010b). This could be explained by the fact that different molecular mechanisms for different cells were used after dust stimulation. The induction of *TNF-α* and *MCP-1*

transcription remarkably increased at 5 μg/100 μL and then unexpectedly decreased, suggesting high level of oxidative stress may inhibit their expression.

Numerous studies have demonstrated a strong correlation between insufficient antioxidant capacity and mitochondrial dysfunction in various cells, which usually triggers event upstream of mitochondrial pathways of apoptosis (Ott et al., 2007). Both epidemiological and experimental evidence found mitochondria seems to be a predominant cellular target for airborne particulate matter (Inoue et al., 2003). Our results showed that housedust caused a significant change in $\Delta\Psi m$ in PHCE cells, which was in accordance with ROS accumulation at a dose-dependent manner. This indicated that the positive correlation observed may be the result of PHCE cellular response to the increased oxidative stress after dust exposure (Yang et al., 2014). Housedust-induced mitochondrial dysfunction in PHCE cells may initiate apoptosis in PHCE cells (Gupta et al., 2013).

In conclusion, the PHCE cells were explored to study housedust-induced cytotoxicity to ocular surface epithelium. Our findings suggested that housedust-induced oxidative stress, inflammation responses and mitochondria dysfunction may pose a risk for human corneal injury. The PHCE cells are an acceptable model to study oxidative injury to ocular surface epithelium, which represents what occurs in vivo to some extent (Deng et al., 2015). However, PHCE cells in present study were monolayer, which was insufficient to mimic *in vivo* cellular functions of stratified corneal epithelium. Therefore, further studies are needed to develop a 3D stratified corneal epithelium model based on PHCE to test dust-induced cytotoxicity in human cornea. Besides, biomarkers used in this study for oxidative damage have their limitations so more specific biomarkers and molecular signal pathway analysis are

414 recommended in future study.

415

Acknowledgements

This work was supported in part by Jiangsu Double-Innovation Program, Jiangsu Innovation Team Program, Jiangsu Provincial Innovation Fund (No. 0211001802) and Graduate Student Innovation Project of Jiangsu Province (No. KYZZ15_0034).

Reference

Apel, K., Hirt, H., 2004. Reactive oxygen species: metabolism, oxidative stress, and signal transduction. Annu. Rev. Plant Biol. 55, 373-399.

Becker, S., Mundandhara, S., Devlin, R.B., Madden, M., 2005. Regulation of cytokine production in human alveolar macrophages and airway epithelial cells in response to ambient air pollution particles: Further mechanistic studies. Toxicol. Appl. Pharmacol. 207, 269-275.

Betts, K.S., 2015. Tracking alternative flame retardants: hand-to-mouth exposures in adults. Environ. Health Perspect. 123, A44.

Black, A.T., Gordon, M.K., Heck, D.E., Gallo, M.A., Laskin, D.L.,Laskin, J.D., 2011. UVB light regulates expression of antioxidants and inflammatory mediators in human corneal epithelial cells. Biochem. Pharmacol. 81, 873-880.

Cao, Y., Bindslev, D.A., Kjaergaard, S.K., 2015. Estimation of the in vitro eye irritating and inflammatory potential of lipopolysaccharide (LPS) and dust by using reconstituted human corneal epithelium tissue cultures. Toxicol. Mech. Methods. 25, 402-409.

Cavet, M.E., Harrington, K.L., Vollmer, T.R., Ward, K.W., Zhang, J.Z., 2011. Anti-inflammatory and anti-oxidative effects of the green tea polyphenol epigallocatechin gallate in human corneal epithelial cells. Mol. Vis. 17, 533-542.

Cejka, C.,Cejkova, J., 2015. Oxidative Stress to the Cornea, Changes in Corneal Optical Properties, and Advances in Treatment of Corneal Oxidative Injuries. Oxid. Med. Cell. Longev. 2015, 591530.

Čejková, J., Štípek, S., Crkovska, J., Ardan, T., Platenik, J., Čejka, C., et al., 2004. UV rays, the prooxidant/antioxidant imbalance in the cornea and oxidative eye damage. Physiol. Res. 53, 1-10.

Cejkova, J., Stipek, S., Crkovska, J.,Ardan, T., 2000. Changes of superoxide dismutase, catalase and glutathione peroxidase in the corneal epithelium after UVB rays. Histochemical and biochemical study. Histol. Histopathol. 15, 1043-1050.

Cree, I.A.,Andreotti, P.E., 1997. Measurement of cytotoxicity by ATP-based luminescence assay in primary cell cultures and cell lines. Toxicol. in Vitro. 11, 553-556.

Cullen, A.P., 2002. Photokeratitis and other phototoxic effects on the cornea and conjunctiva. Int. J. Toxicol. 21, 455-464.

De Saint Jean, M., Baudouin, C., Di Nolfo, M., Roman, S., Lozato, P., Warnet, J.M., et al., 2004. Comparison of morphological and functional characteristics of primary-cultured human conjunctival epithelium and of Wong-Kilbourne derivative of Chang conjunctival cell line. Exp. Eye Res. 78, 257-274.

Deng, R., Hua, X., Li, J., Chi, W., Zhang, Z., Lu, F., et al., 2015. Oxidative Stress Markers Induced by Hyperosmolarity in Primary Human Corneal Epithelial Cells. Plos One. 10, e0126561.

Ekstrand-Hammarstrom, B., Magnusson, R., Osterlund, C., Andersson, B.M., Bucht, A., Wingfors, H., 2013. Oxidative stress and cytokine expression in respiratory epithelial cells exposed to well-characterized aerosols from Kabul, Afghanistan. Toxicol. in Vitro. 27, 825-833.

457 Elner, V.M., Strieter, R.M., Pavilack, M.A., Elner, S.G., Remick, D.G., Danforth, J.M., et al., 1991. Human
458 corneal interleukin-8. IL-1 and TNF-induced gene expression and secretion. Am. J. Pathol. 139,
459 977-988.
460 Fang, M.L., Stapleton, H.M., 2014. Evaluating the Bioaccessibility of Flame Retardants in House Dust
461 Using an In Vitro Tenax Bead-Assisted Sorptive Physiologically Based Method. Environ. Sci.
462 Technol. 48, 13323-13330.
463 Fischer, K.D.,Agrawal, D.K., 2015. Induction of Epithelial-Mesenchymal Transition in House Dust Mite,
464 Ragweed, and Alternaria Sensitized and Challenged Mice. J. Allergy Clin. Immun. 135, AB62.
465 Franck, C.,Skov, P., 1989. Foam at inner eye canthus in office workers, compared with an average Danish
466 population as control group. Acta Ophthalmol. 67, 61-68.
467 Guo, Y.,Kannan, K., 2011. Comparative Assessment of Human Exposure to Phthalate Esters from House
468 Dust in China and the United States. Environ. Sci. Technol. 45, 3788-3794.
469 Gupta, G., Chaitanya, R.K., Golla, M.,Karnati, R., 2013. Allethrin toxicity on human corneal epithelial
470 cells involves mitochondrial pathway mediated apoptosis. Toxicol. in Vitro. 27, 2242-2248.
471 Gupta, S.K., Gupta, S.C., Agarwal, R., Sushma, S., Agrawal, S.S.,Saxena, R., 2007. A multicentric
472 case-control study on the impact of air pollution on eyes in a metropolitan city of India. Indian J.
473 Occup. Environ. Med. 11, 37-40.
474 Hawley, J.K., 1985. Assessment of health risk from exposure to contaminated soil. Risk Anal. 5, 289-302.
475 He, R., Li Y., Xiang P., Li C., Zhou C., Zhang S., et al., 2015. Organophosphorus flame retardants and
476 phthalate esters in indoor dust from different microenvironments: Bioaccessibility and risk
477 assessment. Chemosphere. doi:10.1016/j.chemosphere.2015.10.087.
478 Inoue, M., Sato, E.F., Nishikawa, M., Park, A.M., Kira, Y., Imada, I., et al., 2003. Mitochondrial generation
479 of reactive oxygen species and its role in aerobic life. Curr. Med. Chem. 10, 2495-2505.
480 Kang, Y., Cheung, K.C.,Wong, M.H., 2010a. Polycyclic aromatic hydrocarbons (PAHs) in different indoor
481 dusts and their potential cytotoxicity based on two human cell lines. Environ. Int. 36, 542-547.
482 Kang, Y.A., Cheung, K.C., Wong, M.H., 2010b. The use of cytokine array to examine cytokine profiles of
483 two human cell lines exposed to indoor dust. Toxicol. Lett. 199, 301-307.
484 Kolarik, B., Naydenov, K., Larsson, M., Bornehag, C.G., Sundell, J., 2008. The Association between
485 Phthalates in Dust and Allergic Diseases among Bulgarian Children. Environ. Health Perspect.
486 116, 98-103.
487 Lee, J.B., Kim, S.H., Lee, S.C., Kim, H.G., Ahn, H.G., Li, Z., et al., 2014. Blue Light–Induced Oxidative
488 Stress in Human Corneal Epithelial Cells: Protective Effects of Ethanol Extracts of Various
489 Medicinal Plant Mixtures. Invest. Ophth. Vis. Sci. 55, 4119-4127.
490 Leong, Y.Y.,Tong, L., 2015. Barrier Function in the Ocular Surface: From Conventional Paradigms to New
491 Opportunities. Ocul. Surf. 13, 103-109.
492 Li, H.B., Li, J., Juhasz, A.L., Ma, L.Q., 2014. Correlation of in Vivo Relative Bioavailability to in Vitro
493 Bioaccessibility for Arsenic in Household Dust from China and Its Implication for Human
494 Exposure Assessment. Environ. Sci. Technol. 48, 13652-13659.
495 Liu, S.X., Athar, M., Lippai, I., Waldren, C.,Hei, T.K., 2001. Induction of oxyradicals by arsenic:
496 implication for mechanism of genotoxicity. P. Natl. Acad. Sci. USA. 98, 1643-1648.
497 Lu, L., Reinach, P.S.,Kao, W.W., 2001. Corneal epithelial wound healing. Exp. Biol. Med. 226, 653-664.
498 Mølhave, L., Kjærgaard, S.K., Attermann, J., 2002. Effects in the eyes caused by exposure to office dust.
499 Indoor Air. 12, 165-174.
500 Mølhave, L., Schneider, T., Kjærgaard, S.K., Larsen, L., Norn, S., Jørgensen, O., 2000. House dust in

501 seven Danish offices. Atmos. Environ. 34, 4767-4779.
502 Maertens, R.M., Bailey, J.,White, P.A., 2004. The mutagenic hazards of settled house dust: a review. Mutat.
503 Res-Rev. Mutat. 567, 401-425.
504 Meeker, J.D., Stapleton, H.M., 2010. House dust concentrations of organophosphate flame retardants in
505 relation to hormone levels and semen quality parameters. Environ. Health Perspect. 118, 318-323.
506 Mimura, T., Ichinose, T., Yamagami, S., Fujishima, H., Kamei, Y., Goto, M., et al., 2014. Airborne
507 particulate matter (PM2.5) and the prevalence of allergic conjunctivitis in Japan. Sci. Total
508 Environ. 487, 493-499.
509 Nishida, T., Nakamura, M., Mishima, H., Otori, T.,Hikida, M., 1992. INterleukin 6 facilitates corneal
510 epithelial wound closure in vivo. Arch. Ophthalmol. 110, 1292-1294.
511 Ott, M., Gogvadze, V., Orrenius, S.,Zhivotovsky, B., 2007. Mitochondria, oxidative stress and cell death.
512 Apoptosis. 12, 913-922.
513 Pan, Z., MØLhave, L., KjÆRgaard, S.K., 2000. Effects on Eyes and Nose in Humans after Experimental
514 Exposure to Airborne Office Dust. Indoor Air. 10, 237-245.
515 Pitkäranta, M., Meklin, T., Hyvärinen, A., Paulin, L., Auvinen, P., Nevalainen, A., et al., 2008. Analysis of
516 fungal flora in indoor dust by ribosomal DNA sequence analysis, quantitative PCR, and culture.
517 Appl. Environ. Microb. 74, 233-244.
518 Proulx, S., Landreville, S., Guérin, S.L.,Salesse, C., 2004. Integrin α5 expression by the ARPE-19 cell line:
519 comparison with primary RPE cultures and effect of growth medium on the α5 gene promoter
520 strength. Exp. Eye Res. 79, 157-165.
521 Reuter, S., Gupta, S.C., Chaturvedi, M.M., Aggarwal, B.B., 2010. Oxidative stress, inflammation, and
522 cancer: How are they linked? Free Radical Bio. Med. 49, 1603-1616.
523 Riechelmann, H., Deutschle, T., Grabow, A., Heinzow, B., Butte, W.,Reiter, R., 2007. Differential response
524 of mono mac 6, BEAS-2B, and Jurkat cells to indoor dust. Environ. Health Perspect. 115,
525 1325-1332.
526 Rusyn, I., Kadiiska, M.B., Dikalova, A., Kono, H., Yin, M., Tsuchiya, K., et al., 2001. Phthalates rapidly
527 increase production of reactive oxygen species in vivo: role of Kupffer cells. Mol. Pharmacol. 59,
528 744-750.
529 Saxena, R., Srivastava, S., Trivedi, D., Anand, E., Joshi, S., Gupta, S.K., 2003. Impact of environmental
530 pollution on the eye. Acta Ophthalmol. Scan. 81, 491-494.
531 Shoham, A., Hadziahmetovic, M., Dunaief, J.L., Mydlarski, M.B., Schipper, H.M., 2008. Oxidative stress
532 in diseases of the human cornea. Free Radical Bio. Med. 45, 1047-1055.
533 Spilak, M.P., Madsen, A.M., Knudsen, S.M., Kolarik, B., Hansen, E.W., Frederiksen, M., et al., 2015.
534 Impact of dwelling characteristics on concentrations of bacteria, fungi, endotoxin and total
535 inflammatory potential in settled dust. Build. Environ. 93, Part 1, 64-71.
536 Torricelli, A.A.M., Matsuda, M., Novaes, P., Braga, A.L.F., Saldiva, P.H.N., Alves, M.R., et al., 2014.
537 Effects of ambient levels of traffic-derived air pollution on the ocular surface: Analysis of
538 symptoms, conjunctival goblet cell count and mucin 5AC gene expression. Environ. Res. 131,
539 59-63.
540 Tseng, H.C., Lee, I.T., Lin, C.C., Chi, P.L., Cheng, S.E., Shih, R.H., et al., 2013. IL-1β Promotes Corneal
541 Epithelial Cell Migration by Increasing MMP-9 Expression through NF-κB- and AP-1-Dependent
542 Pathways. Plos One. 8, e57955.
543 Wang, X., Spandidos, A., Wang, H.,Seed, B., 2012. PrimerBank: a PCR primer database for quantitative
544 gene expression analysis, 2012 update. Nucleic Acids Res. 40, D1144-D1149.

Wei, Y.J., Han, I.K., Shao, M., Hu, M., Zhang, J.F.,Tang, X.Y., 2009. PM2.5 Constituents and Oxidative DNA Damage in Humans. Environ. Sci. Technol. 43, 4757-4762.

West, S.K., Bates, M.N., Lee, J.S., Schaumberg, D.A., Lee, D.J., Adair-Rohani, H., et al., 2013. Is Household Air Pollution a Risk Factor for Eye Disease? Inte. J. Env. Res. Pub. Heal. 10, 5378-5398.

Wolkoff, P., Skov, P., Franck, C.,Petersen, L.N., 2003. Eye irritation and environmental factors in the office environment-hypotheses, causes and a physiological model. Scandinavian journal of work, Environ. Health, 411-430.

Wu, W.D, Peden, D.B., McConnell, R., Fruin, S., Diaz-Sanchez, D., 2012. Glutathione-S-transferase M1 regulation of diesel exhaust particle-induced pro-inflammatory mediator expression in normal human bronchial epithelial cells. Part. Fibre Toxicol. 9, 1.

Yang, L., Liu, G., Lin, Z., Wang, Y., He, H., Liu, T., et al., 2014. Pro-inflammatory response and oxidative stress induced by specific components in ambient particulate matter in human bronchial epithelial cells. Environ. Toxicol. doi: 10.1002/tox.22102..

Ye, J., Wu, H., Wu, Y., Wang, C., Zhang, H., Shi, X., et al., 2012. High molecular weight hyaluronan decreases oxidative DNA damage induced by EDTA in human corneal epithelial cells. Eye. 26, 1012-1020.

Yu, B., Wang, Y.,Zhou, Q., 2014. Human health risk assessment based on toxicity characteristic leaching procedure and simple bioaccessibility extraction test of toxic metals in urban street dust of Tianjin, China. Plos One 9, e92459.

Figures

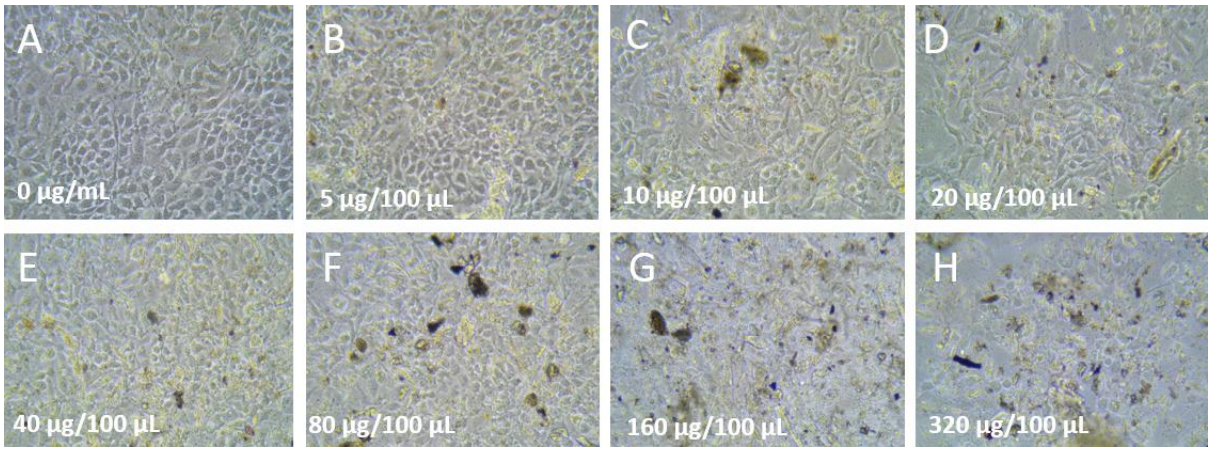

Figure 1 Housedust induced morphology changes of HCE cells following 24 h exposure (magnification 200×). Typical polygonal and cobblestone appearance of confluent HCE cell monolayer was clear in the control group and low exposure group (5 µg/100 µL) (A, B). However, cells became spindle shape with increasing dust concentration (C, D) and cell density was significantly decreased at high exposure groups (> 160 µg/100 µL) (G, H).

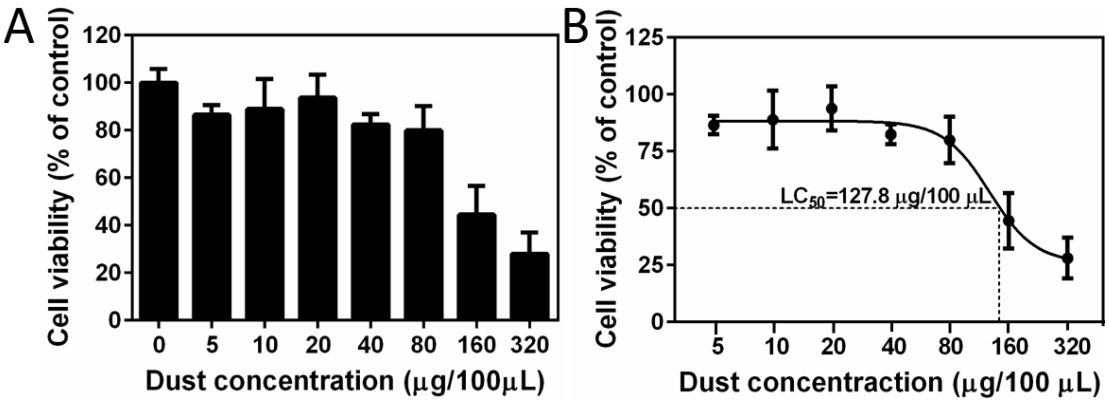

574

575 Figure 2 Concentration-dependent cytotoxicity of housedust in PHCE cells after 24 h
576 exposure. Cell viability was tested by CCK-8 assay to understand dust-induced toxicity to
577 PHCE cells (A). At low concentration, housedust showed little effect on PHCE cells viability
578 (A, B). At higher concentrations (>160 μg/100 μL), the cell viability was remarkably reduced
579 by >50% (A, B). Logarithmic transformation of dust concentration and cell viability data was
580 fit to a nonlinear regression curve (log(agonist) vs response) to calculate LC_{50} (B). Error bar
581 means standard deviation of three replicates.
582

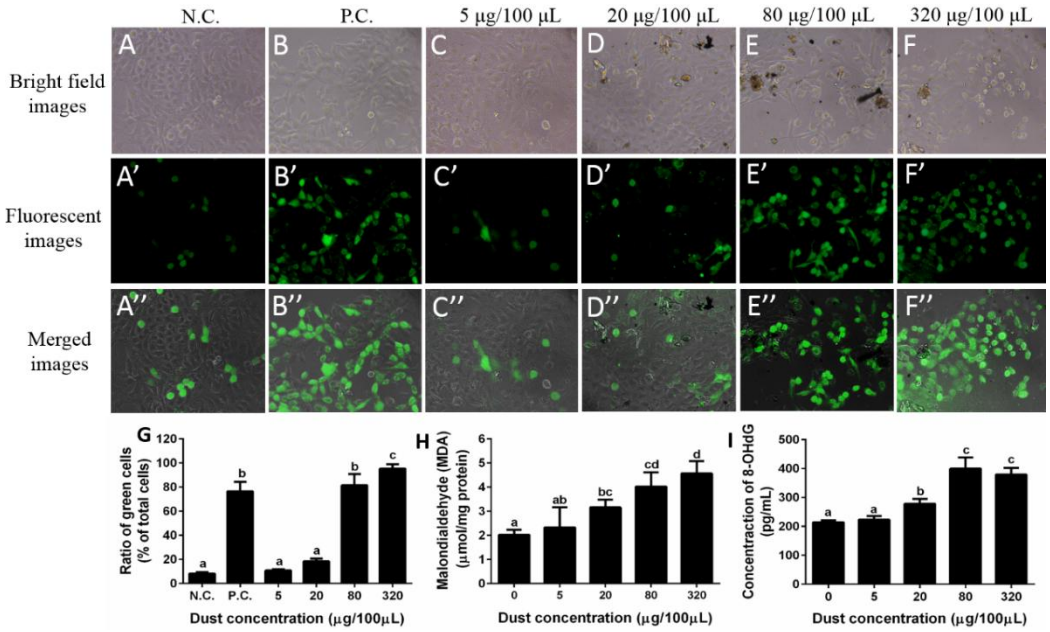

583

584 Figure 3. Housedust-induced oxidative stress in PHCE cells after 24 h exposure with positive
585 and negative control staining. PHCE cells exposed to various concentration of housedust
586 were stained with DCFH-DA probe (magnification 200×) (A'-F'). The PHCE cells after
587 exposing to dust showed a concentration-dependent increase in fluorescence intensity. More
588 than 95% green fluorescent cells was evident after exposure to 160 μg/100 μL dust (A'-F').
589 Green dots indicated ROS positive cells. Ratio of positive cells was recorded (G). Both of
590 MDA (H) and 8-OHdG (I) levels were elevated with increasing dust concentration in PHCE
591 cells, suggesting aggravation of lipid peroxidation and DNA damage. Each bar represents the
592 mean ± SD of three independent experiments. The same letters represent no significant
593 difference at $p<0.05$. NC and PC mean negative and positive control.

594

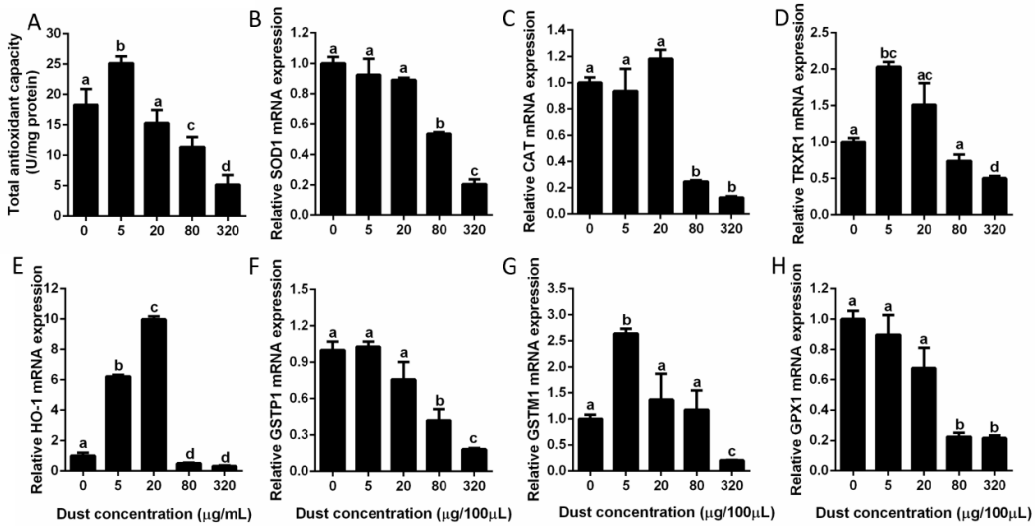

Figure 4. Effects of housedust on total antioxidant capacity (T-AOC) (A) and expression of antioxidant enzyme genes (B-H). HCE cells were treated with various dust concentrations for 24 h. Total RNA was extracted and detected by RT-qPCR. Dust exposure of PHCE cells significantly decreased mRNA expression of *SOD1*, and *CAT* (B and C). For secondary antioxidant enzymes, remarkable up-regulation of *TRXR1* (D), *GSTM1* and *HO-1* (G and E) mRNA were observed, most effective at 5 and 20 μg/100 μL. *GSTP1* and *GPX1* (F and H) mRNA expressions were decreased by 5.6- and 4.8-folds at 320 μg/100 μL. Each bar represents mean ± SD of three replicates. Different letters represent significant difference at $p<0.05$.

606

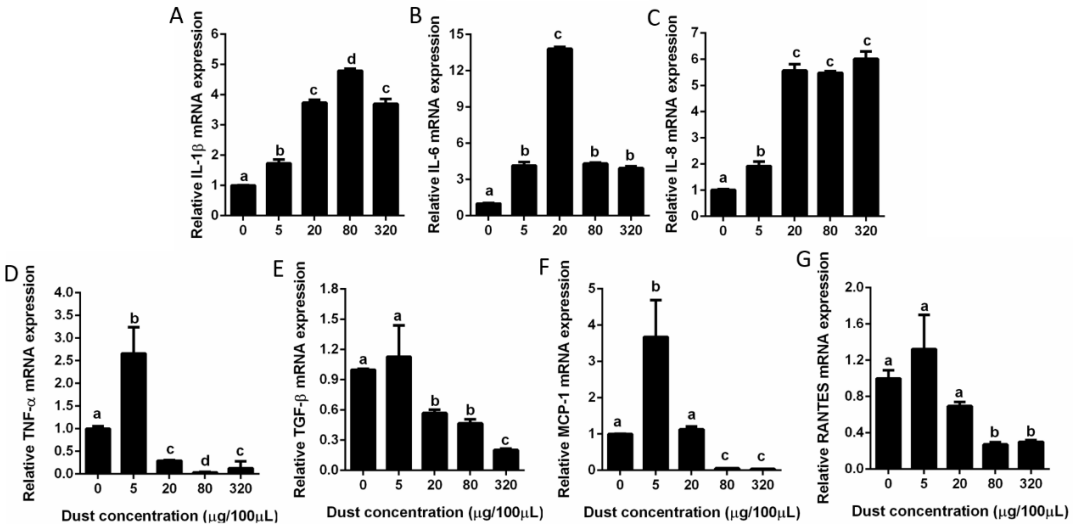

607

608 Figure 5. Housedust-induced expression of inflammatory mediators in HCE cells with dose

609 response. Expression of inflammatory cytokines (*IL-1β, IL-6, TNF-α,* and *TGF-β*) and

610 chemokine *IL-8, MCP-1, RANTES* were measured by RT-qPCR for mRNA levels. Dust

611 caused a dose-dependent increase in mRNA expression of *IL-1β, IL-6 and IL-8* (A, B, and C).

612 Significantly increased mRNA expression of *TNF-α* and *MCP-1* at 2.7–3.7 folds were

613 observed in 5 μg/100 μL dust (E and G). However, 3-fold down-regulation in *TNF-α, MCP-1*,

614 and *RANTES* was evident at > 20 μg/100 μL (H). TGF-β mRNA expression was decreased

615 0.9-4.9 folds in a dose-dependent manner (F). Results are shown as mean ± SD of three

616 replicates. Different letters represent significant difference at $p<0.05$.

617

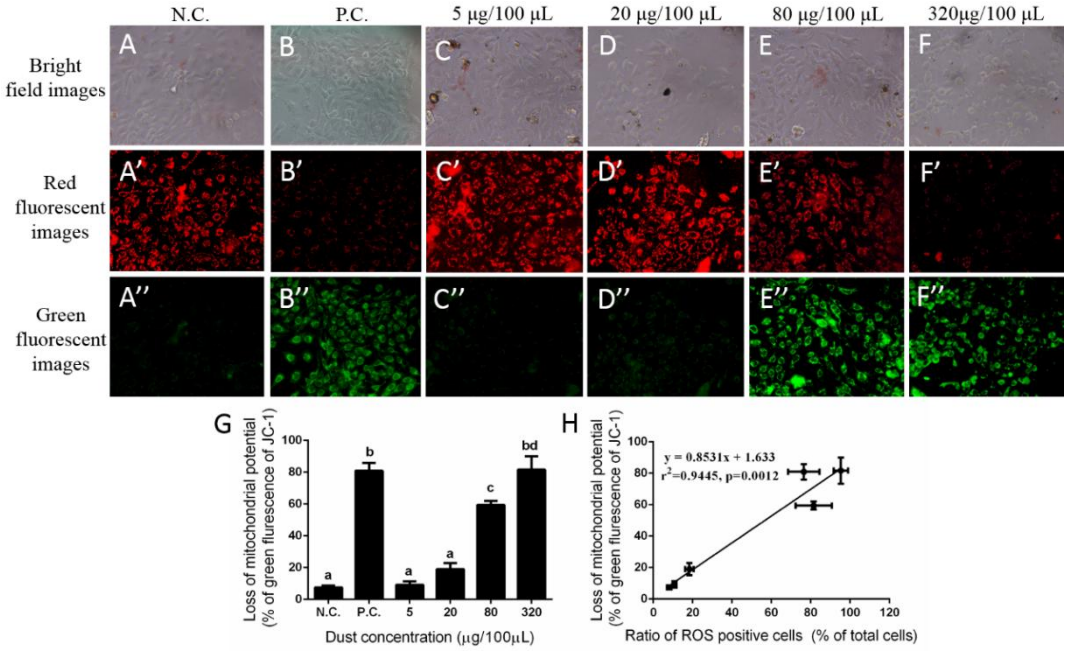

Figure 6. Mitochondrial membrane potential in PHCE cells decreased after exposing to housedust at concentration-dependent manner. PHCE cells were treated with housedust (0, 5, 20, 80, and 320 μg/100 μL) for 24 h, stained with JC-1 and observed by inversed fluorescent microscopy (magnification 200×). After exposure, PHCE cells exhibited an elevated green fluorescence intensity (C''-F'') and an attenuated red fluorescence signal (C'-F') in a dose-dependent manner. The bar diagrams represent the loss of mitochondrial potential (% green fluorescence of JC-1) as detected by flow cytometer (G) and correlation between ROS production and ΔΨm. Data are mean ± SD. N.C. and P.C. mean negative and positive control respectively.

Graphical Abstract

TOC art